

# Neuroprotective Effects of Human Serum Albumin Nanoparticles Loaded With Brimonidine on Retinal Ganglion Cells in Optic Nerve Crush Model

Ko Eun Kim,<sup>1</sup> Inseok Jang,<sup>2</sup> Hyungwon Moon,<sup>2</sup> Yu Jeong Kim,<sup>1</sup> Jin Wook Jeoung,<sup>1</sup> Ki Ho Park,<sup>1</sup> and Hyuncheol Kim<sup>2</sup>

<sup>1</sup>Department of Ophthalmology, Seoul National University Hospital, Seoul National University College of Medicine, Seoul, South Korea

<sup>2</sup>Department of Chemical & Biomolecular Engineering, Sogang University, Mapo-Gu, Seoul, South Korea

Correspondence: Hyuncheol Kim, Department of Chemical & Biomolecular Engineering, Sogang University, 35 Baekbeom-ro, Mapo-Gu, Seoul 121-742, South Korea; hyncheol@sogang.ac.kr.  
Ki Ho Park, Department of Ophthalmology, Seoul National University Hospital, Seoul National University College of Medicine, Seoul, South Korea; kihopark@snu.ac.kr.

KEK and IJ contributed equally to the work presented here and should therefore be regarded as equivalent authors.

Submitted: January 25, 2015

Accepted: July 21, 2015

Citation: Kim KE, Jang I, Moon H, et al. Neuroprotective effects of human serum albumin nanoparticles loaded with brimonidine on retinal ganglion cells in optic nerve crush model.

*Invest Ophthalmol Vis Sci.*

2015;56:5641-5649. DOI:10.1167/iivs.15-16538

**PURPOSE.** We investigated the neuroprotective effect of human serum albumin nanoparticles (HSA-NPs) and their conjugation with brimonidine (HSA-Br-NPs) on retinal ganglion cells (RGCs) in optic nerve crush (ONC) model.

**METHODS.** We fabricated HSA-Br-NPs by ethanol precipitation, including 0.18% brimonidine (Br) and 3.5% human serum albumin (HSA) in HSA-Br-NP solution. We performed ONC and intravitreal injection in Sprague-Dawley rats, which were divided into (1) Normal, (2) balanced salt solution (BSS)-injected ONC, (3) HSA-NP-injected ONC, (4) Br-injected ONC, and (5) HSA-Br-NP-injected ONC groups. Survival of RGC was compared 5 and 14 days after procedures. A cell viability assay evaluated the amyloid- $\beta$  (A $\beta$ )-associated neuroprotective mechanism of HSA-NP.

**RESULTS.** The HSA-Br-NPs showed a narrow size distribution ( $152.8 \pm 51.1$  nm) and a negatively charged surface ( $-29.7 \pm 7.5$  mV), releasing Br for 5 days. The percentages of RGC survival in the HSA-NP ( $52.6 \pm 3.3\%$ ), Br ( $58.0 \pm 4.2\%$ ), and HSA-Br-NP ( $63.5 \pm 7.1\%$ ) groups relative to Normal (100%) were significantly higher than in the BSS group ( $29.2 \pm 3.3\%$ ) 5 days after ONC ( $P < 0.001$ ). However, the HSA-Br-NP ( $38.1 \pm 3.6\%$ ) group showed significantly higher RGC density than the BSS ( $10.3 \pm 5.6\%$ ,  $P < 0.001$ ) or Br ( $18.6 \pm 3.9\%$ ,  $P = 0.006$ ) group at 14 days. The HSA-NP injection reduced A $\beta$  deposition in the RGC layer of ONC model, and a cell viability test showed that HSA-NP can inhibit A $\beta$ -induced RGC death.

**CONCLUSIONS.** Human serum albumin nanoparticles showed neuroprotective potential by inhibiting A $\beta$  deposition, and exerted a sustained therapeutic effect with the combined neuroprotective agent. Our results suggest the potential of HSA-Br-NP as a promising neuroprotective agent.

**Keywords:** human serum albumin-nanoparticle, brimonidine, amyloid beta, retinal ganglion cell, optic nerve crush model

Optic nerve injury induces retinal ganglion cell (RGC) death and subsequent axonal degeneration.<sup>1</sup> A rodent model of optic nerve crush (ONC) injury has shown that gradual death of RGCs occurs within 2 weeks of injury, and involves up to 75% RGC loss.<sup>2</sup> Since damaged neurons cannot regenerate themselves, identifying effective target pathways or proteins that can inhibit apoptotic RGC death is of profound importance to the promotion of their recovery. Such neuroprotective treatment also can be applied to diseases sharing similar pathomechanisms, such as glaucoma, ischemic optic neuropathy, or Alzheimer's disease. However, effective neuroprotective treatment strategies to preserve or regenerate RGCs and their axons still are under investigation.

Brimonidine (Br) is a highly selective  $\alpha_2$ -adrenergic receptor agonist that is well known for its neuroprotective effect against RGC death, which has been confirmed by a large number of experimental studies.<sup>3-9</sup> Brimonidine is known to exert this effect by reducing intraocular excitotoxins (e.g., aspartate, glutamate) elevated secondary to ischemic insult,<sup>10</sup> upregulat-

ing neurotrophic growth factors (e.g., brain-derived neurotrophic factor, fibroblast growth factor),<sup>8,11,12</sup> or activating antiapoptosis cascades,<sup>13,14</sup> ultimately leading to prevention of RGC death. Therefore, continuous and effective delivery of Br to the ganglion cell layers (GCLs) is desired for enhancement of RGC survival.

Previous studies have reported the potential of nanoparticles as an effective intravitreal drug delivery system.<sup>15-17</sup> Among the several types of nanoparticles, the human serum albumin nanoparticle (HSA-NP) has been identified as a promising drug carrier for retinal disease treatment, specifically due to its superior capability in penetrating deeper retinal structures.<sup>15,17</sup> In addition to the advantage of nanoparticles, human serum albumin (HSA) can conjugate to low-molecular-weight drugs or to bioactive proteins and form self-aggregates, thereby facilitating the stable release of intraocular drugs.<sup>18</sup> More importantly, HSA has an innate ability to regulate the accumulation of amyloid- $\beta$  (A $\beta$ ) plaque, which induces

neurodegeneration by deposition of insoluble abnormal aggregates.<sup>19,20</sup>

In light of these findings, we hypothesized that HSA-NPs could have a potential neuroprotective effect as well as drug-delivery capability. Moreover, if HSA-NPs can conjugate with the neuroprotective agent, enhanced effects can be expected. In this regard, we investigated the neuroprotective effects of HSA-NPs and HSA-NPs loaded with Br (HSA-Br-NPs) in an ONC model. The results showed that HSA-NPs, by regulating A $\beta$  aggregation, can be neuroprotective and can enhance the long-term release of delivery drug.

## METHODS

### Materials

We obtained HSA, Br (powder type), ethanol, glutaldehyde solution, and dimethylsulfoxide from Sigma-Aldrich Corp. (St. Louis, MO, USA) and they were used without further purification. Dextran tetramethylrhodamine (DTMR) and Alexa Fluor 555 carboxylic acid succinimidyl ester were purchased from Life Technologies (Carlsbad, CA, USA). Rat A $\beta$  peptide (1-42) was obtained from AnaSpec (Fremont, CA, USA). A Spectra/por dialysis membrane (molecular weight cut-off, 1000) was purchased from Spectrum Labs (Rancho Dominguez, CA, USA), and DAPI was obtained from Invitrogen (Eugene, OR, USA).

### Preparation of HSA-Br-NPs

We synthesized HSA-Br-NPs via the ethanol precipitation method.<sup>21</sup> Specifically, HSA was dissolved in 1 mL distilled water to a final concentration of 20 mg/mL, and Br in dimethylsulfoxide to a final concentration of 10 mg/mL. Subsequently, 200  $\mu$ L Br solution was added to 1 mL HSA solution (20 mg/mL). Ethanol (1.2–3 mL) was added dropwise to the resulting mixture, which then was stirred at 550 rpm for 1 hour on a magnetic stirrer. We added 20  $\mu$ L 4% glutaraldehyde solution to the mixture, which then was stirred overnight at room temperature. After 24 hours of stirring, the HSA-Br-NPs were purified 3 times by centrifugation (16,100g, 10 minutes, 4°C) and then resuspended in distilled water. Finally, the suspension was centrifuged (800g, 5 minutes, 4°C) to remove aggregates.

To prepare HSA-Br-NPs with conjugated NHS-fluorescein, 5  $\mu$ L NHS-fluorescein was added to 1 mL HSA-Br-NP solution, which mixture was maintained at room temperature for 1 hour. To remove the remaining free NHS-fluorescein, the solution was centrifuged (800g, 5 minutes, 4°C) and resuspended twice in a PBS solution (pH 7.4).

To prepare HSA-Br-NPs with conjugated Alexa 555, HSA-Br-NPs were resuspended in PBS (pH 7.4), and Alexa Fluor 555 carboxylic acid succinimidyl ester was dissolved in methanol. Subsequently, 5  $\mu$ L Alexa Fluor 555 carboxylic acid succinimidyl ester solution was added to 1 mL HSA-Br-NP solution. The mixture underwent reaction at room temperature for 30 minutes. To remove the remaining dye, the mixture was centrifuged (800g, 5 minutes, 4°C) and resuspended twice in PBS (pH 7.4).

### Characterization of HSA-Br-NPs

The size distribution and zeta potential of the HSA-Br-NPs that had been suspended in PBS (pH 7.4) at 37°C were measured 3 times on a Malvern Zetasizer Nano ZS 3000HAs (Malvern Instrument Ltd., Worcestershire, UK). Their morphologies were observed by transmission electron microscopy (TEM; CM30, Philips, CA, USA). The HSA-Br-NPs then were dissolved

in distilled water and applied to a 300-mesh copper grid coated with carbon. After 2 minutes, the grid was tapped with filter paper to remove the distilled water and air-dried. Afterward, each grid was stained with a droplet of 2% (wt/vol) uranyl acetate.

To test the *in vitro* release of Br from HSA-Br-NPs, a Spectra/por dialysis membrane (molecular weight cut-off, 1000) was applied. Then, 200  $\mu$ L HSA-Br-NPs was added to the dialysis membrane, both ends of which were sealed with clips. The HSA-Br-NP-loaded membrane then was inserted into a 50-mL tube filled with 50 mL PBS (pH 7.4), and placed in a 37°C shaking incubator. Samples were obtained from the tube at various time points. The amount of Br released from the HSA-Br-NPs was assessed by high-performance liquid chromatography (YL9100 HPLC system; Younglin, Gyeonggi-do, South Korea). Zorbax Eclipse Plus C18 (4.6  $\times$  250 mm, 5  $\mu$ m; Agilent Technologies, Santa Clara, CA, USA) was used for separation. The flow rate was 1.0 mL/min, and elution of the mobile phase of ACN:buffer (10:90; consisting of 10 mM triethylamine adjusted to pH 3.2 with phosphoric acid) was isocratic. The UV detector was set to 248 nm, and the retention time was 6 minutes.

### In Vitro Cellular Uptake of HSA-Br-NPs

We obtained RGC-5 cells (transformed RGC lines) from Alcon Research Lab (Fort Worth, TX, USA), cultured in Dulbecco's modified Eagle's medium containing L-glutamine, and supplemented with 10% fetal bovine serum and 1% penicillin-streptomycin solution (Sigma-Aldrich Corp.). Cells ( $2 \times 10^4$ ) were seeded onto each well of a 12-well plate, at the bottom of which a gelatin-coated cover glass was positioned. After overnight incubation, the cells were treated with HSA-Br-NPs with conjugated NHS-fluorescein, which had been diluted with serum-free medium to a concentration of 10  $\mu$ g/mL. The cells were incubated for 6 and 24 hours. At each time point, they were washed twice with Dulbecco's phosphate buffered saline (DPBS) and fixed with 4% paraformaldehyde for 2 hours. The cells were attached to a gelatin-coated cover glass, which then was mounted by using Vectashield mounting medium with 4',6-diamidino-2-phenylindole (DAPI; Vector Laboratories, Inc., Burlingame, CA, USA). The intracellular uptake of the HSA-Br-NPs was observed under confocal laser scanning microscopy (Leica TCS SP5; Leica Microsystems GmbH, Wetzlar, Germany).

### ONC Injury Model

All of the procedures involving animals adhered to the Association for Research in Vision and Ophthalmology Statement for the Use of Animals in Ophthalmic and Vision Research. Additionally, they were approved by the Animal Research Committee of Seoul National University Hospital. Specifically, male Sprague-Dawley (SD) rats purchased from Koatech (Pyeongtaek, South Korea) and weighing 250 to 300 g were housed with adequate care. Only the right eye of each SD rat was used for all of the procedures. The animals were maintained under alternating dark-light cycles of 12 hours at room temperature. After anesthetization by intramuscular injection of xylazine (1 mg/kg; Rompun, Bayer, Germany) and Zoletil (10 mg/kg; Virbac Animal Health Ltd., Carros, France), the superolateral conjunctiva was incised with scissors. The subconjunctival space was exposed, and the other tissues were separated gently by dissection under surgical microscopy. The optic nerve was exposed, and an aneurysm clip (5.2 mm blade length, 4.0 mm maximal opening, 110 g force; MINI Aneurysm-Clips; Aesculap AG, Tuttlingen, Germany) was used to clip 2 mm behind the globe for 60 seconds, without damaging the retinal perfusion. After

removing the clip, an antibiotic ointment was applied and the animals were allowed to recover.<sup>22</sup>

### Administration of Test Agents

The animals were classified into 5 groups according to the intravitreally administered agent: Normal (normal negative control), BSS-injected ONC, HSA-NP-injected ONC (35  $\mu\text{g}/\mu\text{L}$ ), Br-injected ONC (1.76  $\mu\text{g}/\mu\text{L}$ ), and HSA-Br-NP-injected ONC (35  $\mu\text{g}/\mu\text{L}$  HSA and 1.76  $\mu\text{g}/\mu\text{L}$  Br) rat groups. Each group comprised at least 5 rats. The calculated concentration of Br in the HSA-Br-NP solution was 0.18% (wt/vol). Immediately following the ONC procedure, an equal amount (5  $\mu\text{L}$ ) of each agent was administered intravitreally by Hamilton syringe (Hamilton Company, Reno, NV, USA).

### Quantification of RGCs

To evaluate the RGC count 5 days after the ONC procedure and injection, retrograde labeling with DTMR (Molecular Probes, Eugene, OR, USA) was performed one day before enucleation. We applied DTMR to the proximal cut surface of the optic nerve. Five days post ONC and injection, the eyes were enucleated and fixed with 4% paraformaldehyde solution at 4°C for 120 minutes ( $n \geq 5$  per group). The retinas were dissected, flattened with 4 radial cuts, and flat-mounted whole on glass slides. The slides were maintained in the dark and air-dried overnight. The DTMR-labeled RGCs were examined under fluorescence microscopy (BX-61; Olympus, Tokyo, Japan), and fluorescence micrographs were obtained with a microscope eyepiece reticle ( $\times 400$  final magnification) 1, 2, and 3 mm from the center of the optic nerve along the centerline of each retinal quadrant. Labeled RGCs in the fluorescence micrographs were counted in a masked fashion by 3 independent investigators (IJ, KEK, and YJK), and the results were averaged. To calculate the mean density of labeled RGCs per square millimeter of each retina, the number of labeled cells in the 12 photographs was divided by the area of the region. The same procedures were repeated for evaluation of RGC survival 14 days post ONC and intravitreal injection.

### In Vivo Distribution of HSA-Br-NPs in Retina

A total of 5  $\mu\text{L}$  HSA-Br-NPs labeled with Alexa 555 in PBS (35  $\mu\text{g}/\mu\text{L}$  HSA and 1.76  $\mu\text{g}/\mu\text{L}$  Br, pH 7.4) was intravitreally injected using a Hamilton syringe (Hamilton Company). At 6, 24, and 72 hours after injection, the eyes were enucleated and fixed in 4% paraformaldehyde for 24 hours ( $n \geq 5$  per group). They then were embedded in 7% agarose gel with 0.2% sodium azide and sliced to 200  $\mu\text{m}$  thickness using a vibratome section. The slices were stained with 0.01% DAPI/PBTA solution (0.5% BSA, 0.05% sodium azide, and 0.1% Triton X-100 in PBS) overnight. After staining, the slices were washed with fresh PBTA 3 times and then mounted with Vectashield mounting medium (Vector Laboratories, Inc.). The retinal distribution of the HSA-Br-NPs was observed under confocal laser scanning microscopy (Leica Microsystems GmbH).

### Immunohistochemical Staining of A $\beta$

The SD rats were divided into 3 groups: normal, ONC model, and HSA-NP-injected ONC model ( $n = 4$  per each group). Right eyes were enucleated 14 days after the procedures and then immersed in 4% paraformaldehyde for 24 hours. They then were embedded in 7% agarose gel with 0.2% sodium azide and sliced to 200  $\mu\text{m}$  thickness using a vibratome section. The slices were treated with anti-A $\beta$  (1-40), a rabbit antibody (Merck Millipore, Darmstadt, Germany), which had been

diluted to 1/100 in PBTA. After 24 hours, the slices were washed with PBTA 3 times and treated with a 1:100 solution of Alexa Fluor 488 goat anti-rabbit IgG (Molecular Probes) and 0.01% DAPI in PBTA. After 24 hours, the samples were washed with PBTA 3 times and mounted with Vectashield mounting medium (Vector Laboratories, Inc.). The presence of A $\beta$  in the retinal layers of the ONC model was examined under confocal laser scanning microscopy (Leica Microsystems GmbH).

### Cell Viability Assay for HSA Inhibition of A $\beta$ Neurodegeneration Mechanism

To identify the mechanism of HSA inhibition of A $\beta$  neurodegeneration, cell viability was evaluated by reduction assay using 3-(4,5-dimethylthiazol-2-yl)-2,5-diphenyltetrazolium bromide (MTT; Roche Applied Science, Indianapolis, IN, USA). We seeded RGC-5 cells ( $2 \times 10^4$  per well) in 96-well plates. At 24 hours after plating, the cells were treated separately with A $\beta$  (20  $\mu\text{M}$ ), HSA-NP (30  $\mu\text{g}/\mu\text{L}$ ), and A $\beta$  (20  $\mu\text{M}$ ) mixed with HSA-NP (30  $\mu\text{g}/\mu\text{L}$ ; 5 wells per each group). After incubations for various durations (12, 24, and 48 hours), the wells were washed with  $1 \times$  DPBS, and 30  $\mu\text{L}$  MTT and distilled water (3 mg/mL) were added. The wells then were incubated for 4 hours at 37°C, after which 100  $\mu\text{L}$  DMSO was added before measurement with a plate reader (EL800; BioTek Instruments, Inc., Winooski, VT, USA).

### Statistical Analysis

The data are presented as means with standard deviations of at least 3 independent experiments. A 1-way ANOVA with post hoc Tukey test was conducted to compare the groups' RGC densities in in vivo and cell viability experiments. All of the statistical analyses were performed using SPSS version 21.0 for Windows (IBM Corp., Armonk, NY, USA). Statistical significance was determined to be  $P < 0.05$ .

## RESULTS

### Characterization of Nanoparticles

Zetasizer measurements revealed that the HSA-Br-NPs had a uniform size distribution ( $152.8 \pm 51.1$  nm diameter) and highly negative potential ( $-29.7 \pm 7.5$  mV; Fig. 1A). The TEM image in Figure 1B shows a round shape and a narrow size distribution. The HSA-Br-NPs released an accumulated quantity of Br ranging from  $107.13 \pm 4.18$  to  $214.12 \pm 0.43$   $\mu\text{g}$ , which continuously increased with time (Fig. 1C).

### In Vitro and In Vivo Distribution of HSA-Br-NPs

The in vitro cellular distribution of NHS-fluorescein-conjugated HSA-Br-NPs was observed under confocal laser-scanning microscopy. Merged images showed localization in the RGC-5 cells at 6 and 24 hours after HSA-Br-NP treatment (Fig. 2). These results indicated good intracellular uptake of HSA-Br-NPs.

Figure 3 plots the retinal distributions of HSA-NPs in normal control (Fig. 3A) and ONC model (Fig. 3B) at baseline, and 6, 24, and 72 hours after injection ( $n \geq 5$ ). Their persistent time and distribution patterns in the retinal layer did not differ between the 2 groups. Images with DAPI and Alexa 555 reveal the locations of the retinal layers and HSA-Br-NPs, respectively. Merged images confirmed that the HSA-Br-NPs were located within the retinal layers. The magnified images in Figure 3 further demonstrated that the HSA-Br-NPs were well located within the GCL.

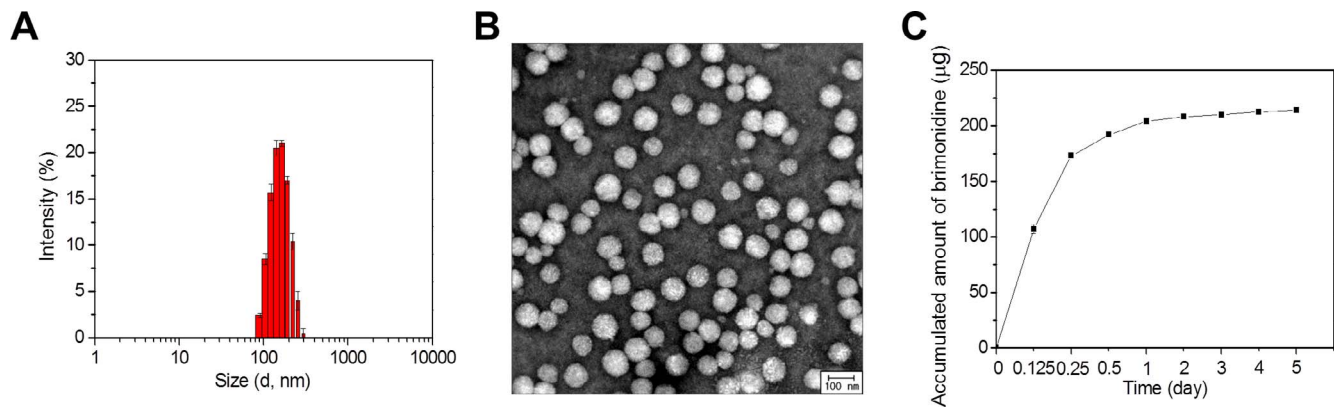


**FIGURE 1.** Characterization of HSA-Br-NPs. (A) Particle size was measured using Zetasizer. (B) The TEM image of HSA-Br-NPs showing particles of round shape and narrow size distribution ( $152.8 \pm 51.1$  nm diameter). Scale bar: 100 nm. (C) In vitro data showing accumulated amount of Br released from HSA-Br-NPs, which continuously increased with time.

### Effect of HSA-Br-NPs on RGC Survival in ONC Model

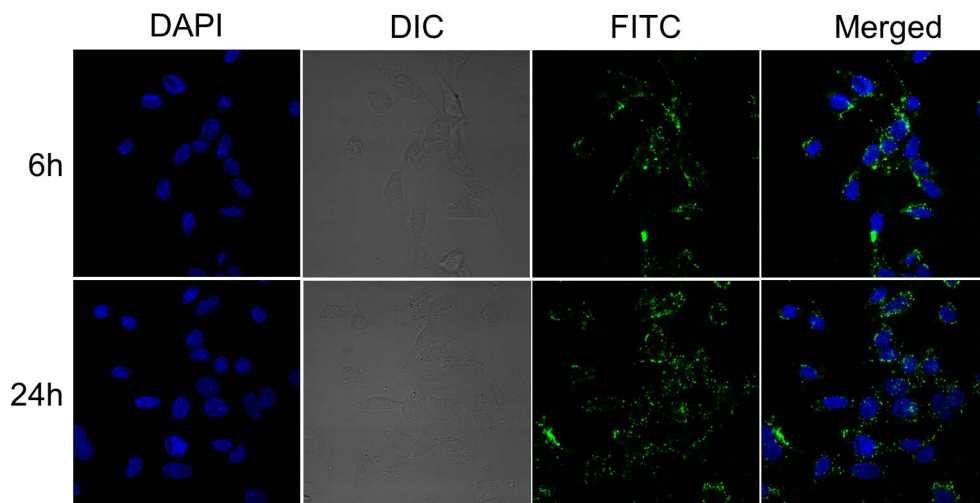
#### Model

Figure 4A shows the remaining RGCs in the groups at 5 (first row) and 14 (second row) days following the procedure and the Table summarizes their densities. The percentages of RGC survival relative to the RGC density in the Normal group (100%) were  $29.2 \pm 3.3$ ,  $52.6 \pm 3.3$ ,  $58.0 \pm 4.2$ , and  $63.5 \pm 7.1\%$  in the BSS, HSA-NP, Br, and HSA-Br-NP groups, respectively, at 5 days, and  $10.3 \pm 5.6$ ,  $30.7 \pm 11.7$ ,  $18.6 \pm 3.9$ , and  $38.1 \pm 3.6\%$ , respectively, at 14 days (Fig. 4B). The RGC densities at 5 and 14 days after ONC injury and intravitreal injection then were compared among the BSS, HSA-NP, Br, and HSA-Br-NP groups to evaluate their neuroprotective effects. Five days after the procedure, the RGC densities in the HSA-NP ( $P < 0.001$ ), Br ( $P < 0.001$ ), and HSA-Br-NP ( $P < 0.001$ ) groups were significantly higher than that in the BSS group. However, 14 days after the procedure, only the HSA-NP ( $P = 0.002$ ) and HSA-Br-NP ( $P < 0.001$ ) groups showed significantly higher RGC densities than the BSS group. When comparing the Br and HSA-Br-NP groups, there was no significant difference at 5 days ( $P = 0.015$ ); however, at 14 days, the HSA-Br-NP group showed a significantly higher RGC density ( $P = 0.006$ ).

### Neuroprotective Mechanism of HSA-NPs

To investigate the possible pathogenic role of A $\beta$  in RGC apoptosis and the therapeutic effect of HSA-NP against A $\beta$ , we examined the presence of A $\beta$  aggregation in the ONC model and performed an MTT assay. The immunohistochemistry results showed elevated expression of A $\beta$  in the GCL of the ONC model relative to the normal rats at 14 days following injury (Fig. 5). Merged DAPI and FITC images revealed the locations of A $\beta$  in the retinal layers, and a magnified image indicated that A $\beta$  was specifically located in the GCL. Interestingly, the amount of A $\beta$  deposition was lower in the GCL of the HSA-NP-injected ONC model than in that of the ONC-only model.

An in vitro experiment showed that the respective RGC viabilities in the groups treated with HSA-NPs, A $\beta$  with HSA-NPs, and A $\beta$  relative to that in the nontreated control group (100%) were  $98.5 \pm 4.0$ ,  $90.0 \pm 11.6$ , and  $78.1 \pm 8.2\%$  at 12 hours;  $94.9 \pm 7.6$ ,  $86.4 \pm 7.8$ , and  $65.6 \pm 7.7\%$  at 24 hours; and  $89.9 \pm 4.9$ ,  $71.9 \pm 8.5$ , and  $51.9 \pm 7.6\%$  at 48 hours (Fig. 6). In addition, at 48 hours, the RGC-5 cell viability was significantly decreased in the A $\beta$  group relative to the control ( $P < 0.001$ ) and HSA-NP ( $P < 0.001$ ) groups; however, the A $\beta$



**FIGURE 2.** In vitro cellular uptake of HSA-Br-NPs by RGC-5 cells at 6 and 24 hours after treatment with HSA-Br-NPs. The DAPI, DIC, and FITC images represent the location of the RGC-5 cells' nucleus, cell membranes, and the location of the HSA-Br-NPs, respectively. Merged images confirmed that the HSA-Br-NPs were well-penetrated within the RGC-5 cells. All of the images were taken at the same final magnification level ( $\times 1000$ ).

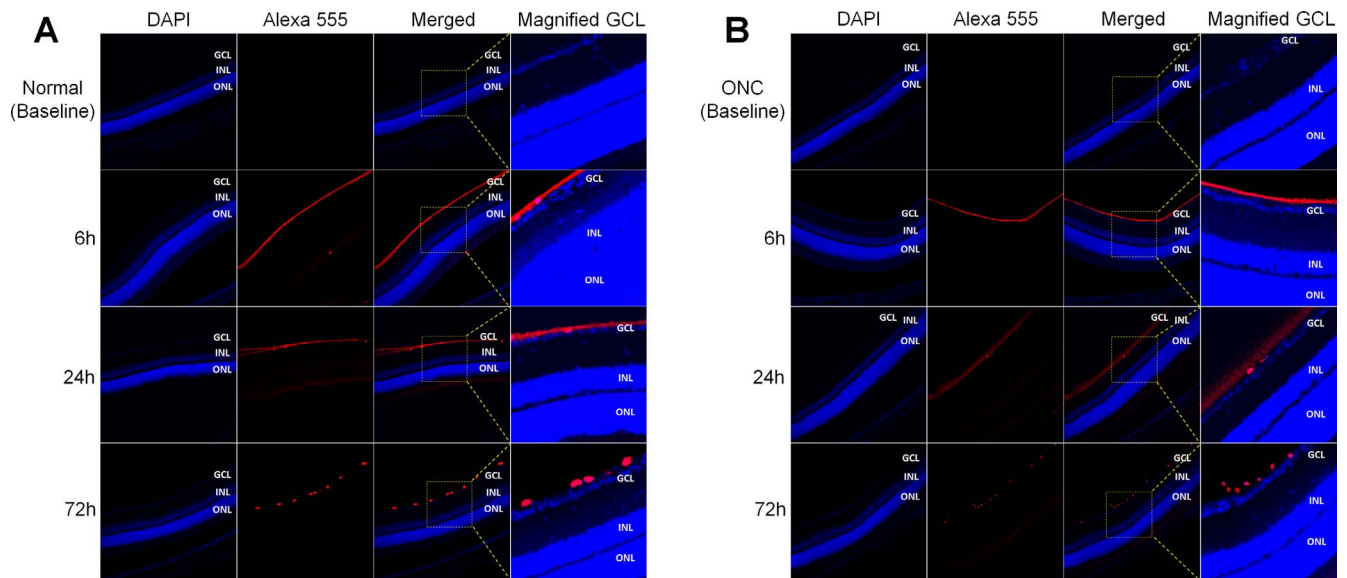


**FIGURE 3.** In vivo retinal distribution of HSA-Br-NPs in (A) normal rat and (B) ONC model at baseline and 6, 24, and 72 hours after intravitreal injection of HSA-Br-NPs ( $n \geq 5$  per group at each time point). Images with DAPI and Alexa 555, respectively, represent the location of the retinal cells' nucleus and the location of the HSA-Br-NPs. Magnified GCL images confirmed that the HSA-Br-NPs were colocalized within the GCL among the intraretinal layers at 6, 24, and 72 hours after injection. All of the images were taken at the same final magnification level ( $\times 150$ ). INL, inner nuclear layer; ONL, outer nuclear layer.

and HSA-NP cotreated group showed significantly higher RGC viability than the A $\beta$  group ( $P = 0.012$ ).

## DISCUSSION

Nanoparticles have been anticipated to have promising therapeutic roles in many diseases, including glaucoma<sup>23</sup> and optic neuropathy.<sup>24</sup> Among the several types of nanoparticles, HSA-NP has been reported to have a beneficial potential as an intraocular therapeutic modality.<sup>15,17</sup> Moreover, in consideration of HSA's neuroprotective effect by elimination of A $\beta$ ,<sup>19,20</sup> we speculated that HSA-NP could synergistically enhance neuronal cell survival and deliver neuroprotective drugs. Hence, we investigated the neuroprotective effect of HSA-NP on RGC survival in the ONC model. More pertinently, the potential of HSA-NP as an effective drug carrier when combined with Br, a known neuroprotective drug, was examined. The present study demonstrates that HSA-NPs attenuate RGC loss by regulating A $\beta$  aggregation and can enhance the beneficial effect of Br.

For intravitreally injected nanoparticles to fulfill their role as an intraocular drug delivery system, they must overcome several barriers that hamper them from targeting the specific site of action. The important physical barriers against macromolecular penetration of the subretinal space are the vitreous and retinal layers, especially the internal limiting membrane and external limiting membrane.<sup>25</sup> First, the vitreous network has a negative potential, for it consists of collagen and hyaluronic acid.<sup>26</sup> Koo et al.<sup>15</sup> reported that NPs with negative potential, such as HSA-NP and hyaluronic acid-NP, were observed throughout the entire retinal layers, while polyethyleneimine-NP, with a positive potential, was trapped in the vitreous until 72 hours post intravitreal injection. Our HSA-Br-NPs also had a negative surface charge ( $-29.7 \pm 7.5$  mV) similar to that of HSA-NP in a previous study,<sup>15</sup> enabling them to easily pass the vitreous. Second, the size of the HSA-Br-NP is approximately 150 nm, which is relatively larger than the pore size of internal limiting membrane (10 to 20 nm)<sup>27</sup> and external limiting membrane (3 to 3.6 nm).<sup>28</sup> Therefore, it

would be impossible for HSA-Br-NP to overcome the retinal layers just by diffusion. We hypothesized that HSA-NPs would have to penetrate through the retinal layers by receptor-mediated endocytosis, as suggested elsewhere.<sup>29</sup> One of the known HSA-binding receptors is the TGF $\beta$  receptor,<sup>30,31</sup> which also is expressed on the surface of RGCs and Müller cells. Previous results showing colocalization of Müller cells and HSA-NPs also might support our theory.<sup>15,17</sup> Therefore, we assumed that TGF $\beta$  could be one of the candidate receptors for the endocytosis of HSA-Br-NPs in the retinal layers, though further experiments are warranted for confirmation. Nevertheless, intravitreal injection of HSA-NP is expected to surmount intraocular barriers to exhibit neuroprotection and to deliver targeting agent to the aiming site.

In this study, Br was chosen as a neuroprotective drug to be loaded into the hydrophobic pockets of HSA-NPs, for the following reasons. First, it is one of the best known and most widely used neuroprotective drugs, and can benefit from nanomedicine technology by increasing the contact time with the ganglion cell layer.<sup>32</sup> Second, it is a hydrophobic compound that has features similar to those of other drugs (e.g., paclitaxel), that have been formulated into albumin-nanoparticles for use in targeted drug delivery systems.<sup>18,33</sup> Additionally, Br can be entrapped in a protein structure and be cross-linked to glutaraldehyde.<sup>21</sup>

In the present study, Br, HSA-NP, and HSA-Br-NP showed neuroprotective capabilities in the ONC model 5 days after ONC injury. Interestingly, HSA-NP itself showed significant improvement in RGC survival in the ONC model relative to the BSS group. Previous studies have reported the pathogenic role of A $\beta$  aggregation in neurodegenerative disease<sup>20,34,35</sup> and glaucoma,<sup>36</sup> as well as the capability of HSA-inhibiting A $\beta$  plaque formation by regulation of A $\beta$  fibril growth.<sup>20</sup> Our immunohistochemistry results indicated positive A $\beta$  expression in the GCL of the ONC model, which expression was decreased by the intravitreal injection of HSA-NP. Moreover, the RGC-5 cell viability test showed increased cell survival by the addition of HSA-NP to A $\beta$  compared to that with A $\beta$ . Consistent with previous studies, the neuroprotective effect of HSA-NP on

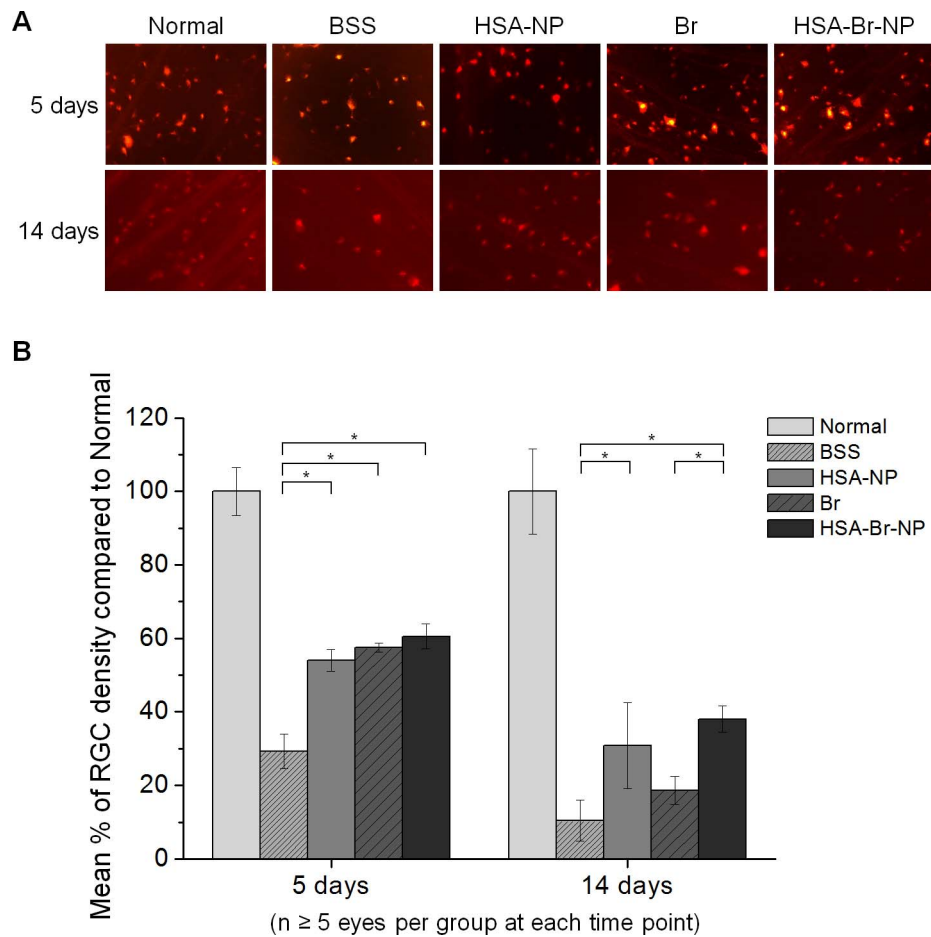


**FIGURE 4.** Effect of HSA-Br-NPs on survival of RGCs in ONC injury model. Animals were classified into 5 groups according to the intravitreally administered agents: (1) Normal control, (2) BSS-injected ONC, (3) HSA-NP-injected ONC, (4) Br-injected ONC, and (5) HSA-Br-NP-injected ONC rat groups. The RGC density in each group was evaluated 5 and 14 days after the ONC procedure and intravitreal injection ( $n \geq 5$  per group at each time point). (A) Fluorescent retinal flat mount images showing remnant RGCs in each group at 5 and 14 days. All of the images were taken at the same final magnification level ( $\times 400$ ). (B) In comparing the RGC densities among the groups, the HSA-NP ( $P < 0.001$ ), Br ( $P < 0.001$ ), and HSA-Br-NP ( $P < 0.001$ ) groups showed higher RGC densities than the BSS group 5 days post ONC. However, 14 days after the procedure, only the HSA-NP ( $P = 0.002$ ) and HSA-Br-NP ( $P < 0.001$ ) groups showed significantly higher RGC densities than the BSS group. Additionally, a significantly higher RGC density was found in the HSA-Br-NP group than in the Br group at 14 days ( $P = 0.006$ ). All comparisons were performed using 1-way ANOVA with post hoc Tukey test ( $^*P < 0.013$ ; 0.05 divided by 4).

RGC survival was most likely to be via regulation of A $\beta$  aggregation. Further studies are needed to investigate the detailed mechanism (e.g., direct elimination of A $\beta$  or inhibition of A $\beta$  plaque formation) of HSA-NP with intraocular A $\beta$  or other possible mechanisms.

One of the primary goals of a nanoparticle drug-delivery system is to make possible continuous long-term treatment. In

**TABLE.** Retinal Ganglion Cell Survival Densities (the Mean Number of Cells/mm<sup>2</sup>  $\pm$  SD) in Each of the (1) Normal Control, (2) BSS-Injected ONC, (3) HSA-NP-Injected ONC, (4) Br-Injected ONC, and (5) HSA-Br-NP-Injected ONC Rat Groups

Groups	Retinal Ganglion Cell Densities	
	5 d After ONC	14 d After ONC
Normal	1501.3 $\pm$ 98.1	2236.2 $\pm$ 258.3
BSS	438.3 $\pm$ 69.7	232.4 $\pm$ 126.0
HSA-NP	810.9 $\pm$ 45.8	688.3 $\pm$ 262.3
Br	862.7 $\pm$ 18.4	415.0 $\pm$ 86.8
HSA-Br-NP	908.8 $\pm$ 51.4	851.2 $\pm$ 80.6

the present study, the therapeutic effect of the HSA-NP and HSA-Br-NP groups lasted longer than those of the other groups. The RGC density was similar between the Br and HSA-Br-NP groups at 5 days, but the HSA-Br-NP group showed higher RGC density at 14 days. Interestingly, the HSA-Br-NP group showed the strongest therapeutic effect at 14 days after ONC. We assumed that the HSA-NPs probably enabled the longer intraocular availability of Br by supporting the sustained release of Br, as in our *in vitro* release test. Moreover, the original neuroprotective effect of Br probably has synergistically supported the therapeutic effect of HSA-NP, enabling a longer and stronger neuroprotective effect of HSA-Br-NP than HSA-NP or Br only. However, despite their therapeutic effect lasting up to 14 days, the HSA-Br-NPs were detected for 3 days, but not for 5 days (data not shown) in the retinal layers of either the normal control or the ONC model. For the discrepancy between the presence of HSA-Br-NPs in the retinal layers and the effect time, we assumed that because the HSA-NPs' A $\beta$  elimination effect was added to the therapeutic effect of Br, the HSA-Br-NPs could have exhibited an augmented initial neuroprotective effect relative to that of pure Br. Therefore, even under the scenario of total HSA-Br-NP

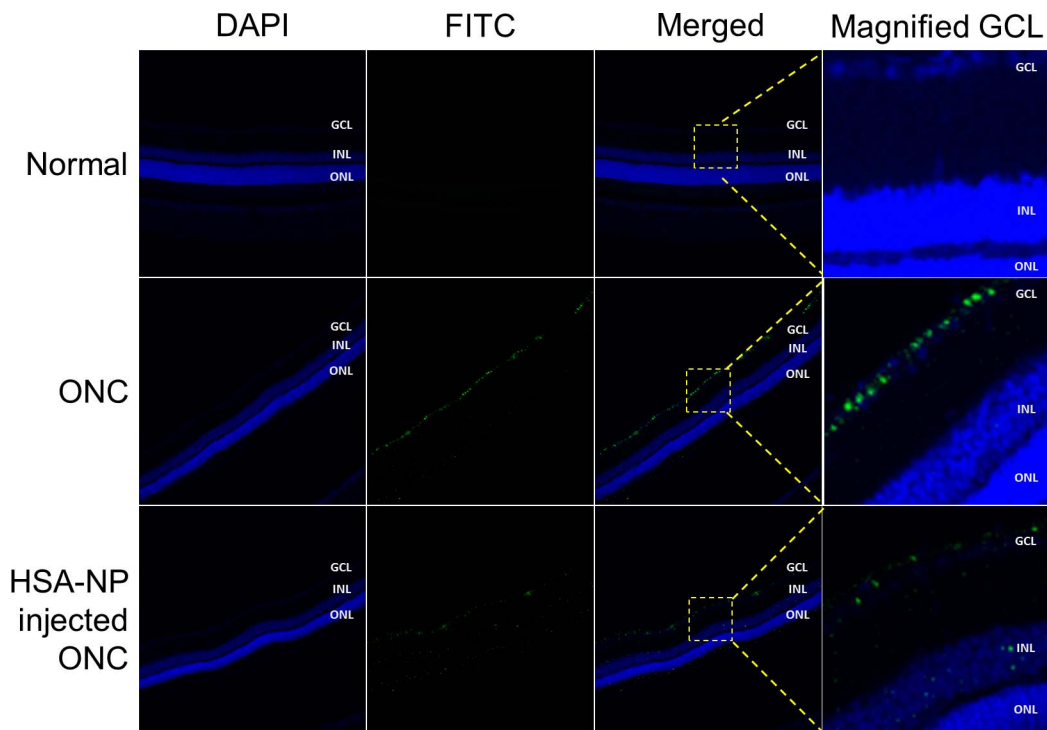


**FIGURE 5.** Immunohistochemistry for Aβ in the retinal layers of normal rat, ONC model, and ONC model injected with HSA-NPs 14 days after ONC injury and intravitreal injection (all  $n = 4$ ). The DAPI and FITC images represent the location of the retinal cells' nucleus and of Aβs, respectively. Merged images show the location of Aβs in the retinal layers. The magnified GCL images also confirm that the Aβs were expressed in the GCL of the ONC model. According to the magnified GCL images, the amount of Aβ deposition was decreased in the HSA-NP-injected ONC model than that in the ONC-only model. All of the images were taken at the same final magnification level ( $\times 150$ ).

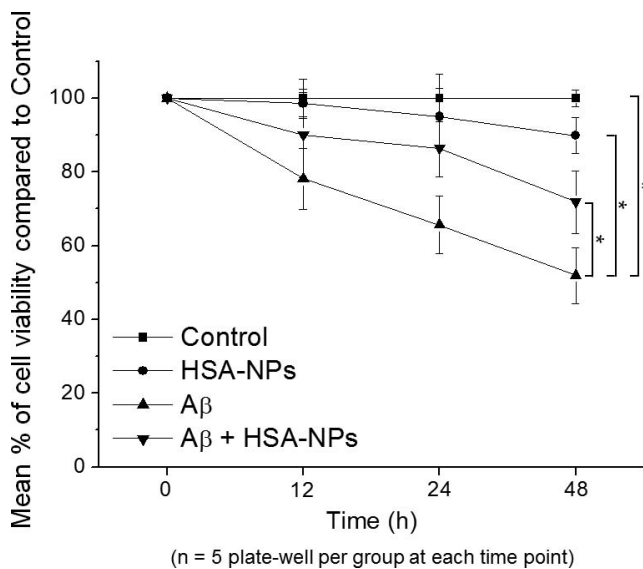


**FIGURE 6.** Neuroprotective mechanism of HSA-NPs against Aβ. The cell viability assay was examined under 3 different conditions—treated with HSA-NP, Aβ, and HSA-NP with Aβ—as compared to the normal control group at 12, 24, and 48 hours after treatment (each group of 5 wells). At 48 hours after treatment, the RGC-5 cell viability was significantly decreased in the Aβ group in comparison with the control group ( $P < 0.001$ ) and the HSA-NP group ( $P < 0.001$ ). However, the Aβ and HSA-NP cotreated group showed significantly higher RGC viability than did the Aβ group ( $P = 0.012$ ). All comparisons were performed using 1-way ANOVA with post hoc Tukey test ( $^*P < 0.013$ ; 0.05 divided by 4).

degradation before 14 days, a latent period with respect to reactivation of the apoptotic pathways or accumulation of Aβ could have existed, consequently showing the reduced Aβ deposition amount until 14 days. Further efforts to extend the persistent time of HSA-NP are warranted for the purposes of their potential application to general treatments.

Our study has several limitations. First, RGC-5 cells were used for in vitro experiments. We did test some of the reliable RGC markers, and our RGC-5 cells showed positive Brn3a and Thy1 expression (data not shown), indicating that these have an RGC-like nature. However, due to their inherent limitation,<sup>37,38</sup> further in vitro experiments with primary retinal culture cell lines from rats should be performed to confirm our in vivo results. Second, the neuroprotective effect of Br was not investigated separately in the present study. Injury to the ONC has been reported to induce RGC apoptosis associated with caspase-2, -3, -9, and Bax,<sup>39,40</sup> and Br is known to potentially attenuate RGC loss by activating antiapoptotic proteins, such as bcl-2 and bcl-xl.<sup>9</sup> Because such neuroprotective mechanisms of Br in the ONC model already have been reported, and also because a similar ONC model was used in this study, we assumed that Br would exert its neuroprotective effect through the identified pathway. However, the possibility of Br's different neuroprotective mechanism under the condition of its coexistence with HSA-NP remains. Therefore, further separate experiments with Br, HSA-NP, and HSA-Br-NP should be performed to investigate each agent's original mechanism of neuroprotection.

In conclusion, HSA-NPs showed a neuroprotective effect in the ONC model as well as a capacity to deliver ocular drugs to the GCL. Moreover, HSA-NPs loaded with Br exerted a longer therapeutic effect and synergistically enhanced the neuroprotectivity. Therefore, HSA-Br-NPs, having the potential to enhance the survival of RGCs, can be considered as a

candidate neuroprotective agent for treatment in optic neuropathies.

### Acknowledgments

Supported by Grant 34-2013-0090 from the SK Telecom Research Fund and Grant HI13C2061 from the Korea Health Technology R&D Project, Ministry of Health & Welfare, Korea, and by the Basic Science Research Program through the National Research Foundation of Korea (NRF) and the Ministry of Education, Science and Technology (NRF-2013R1A2A2A04015829 and NRF-2011-0009606).

Disclosure: **K.E. Kim**, None; **I. Jang**, None; **H. Moon**, None; **Y.J. Kim**, None; **J.W. Jeoung**, None; **K.H. Park**, None; **H. Kim**, None

### References

- Yoles E, Schwartz M. Degeneration of spared axons following partial white matter lesion: implications for optic nerve neuropathies. *Exp Neurol*. 1998;153:1-7.
- Levkovitch-Verbin H, Harris-Cerruti C, Groner Y, Wheeler LA, Schwartz M, Yoles E. RGC death in mice after optic nerve crush injury: oxidative stress and neuroprotection. *Invest Ophthalmol Vis Sci*. 2000;41:4169-4174.
- Lafuente MP, Villegas-Perez MP, Sobrado-Calvo P, Garcia-Aviles A, Miralles de Imperial J, Vidal-Sanz M. Neuroprotective effects of alpha(2)-selective adrenergic agonists against ischemia-induced retinal ganglion cell death. *Invest Ophthalmol Vis Sci*. 2001;42:2074-2084.
- Lafuente Lopez-Herrera MP, Mayor-Torroglosa S, Miralles de Imperial J, Villegas-Perez MP, Vidal-Sanz M. Transient ischemia of the retina results in altered retrograde axoplasmic transport: neuroprotection with brimonidine. *Exp Neurol*. 2002;178:243-258.
- Aviles-Trigueros M, Mayor-Torroglosa S, Garcia-Aviles A, et al. Transient ischemia of the retina results in massive degeneration of the retinectal projection: long-term neuroprotection with brimonidine. *Exp Neurol*. 2003;184:767-777.
- Mayor-Torroglosa S, De la Villa P, Rodriguez ME, et al. Ischemia results 3 months later in altered ERG, degeneration of inner layers, and deafferented tectum: neuroprotection with brimonidine. *Invest Ophthalmol Vis Sci*. 2005;46:3825-3835.
- Ortin-Martinez A, Valiente-Soriano FJ, Garcia-Ayuso D, et al. A novel in vivo model of focal light emitting diode-induced cone-photoreceptor phototoxicity: neuroprotection afforded by brimonidine, BDNF, PEDF or bFGF. *PLoS One*. 2014;9:e113798.
- Gao H, Qiao X, Cantor LB, WuDunn D. Up-regulation of brain-derived neurotrophic factor expression by brimonidine in rat retinal ganglion cells. *Arch Ophthalmol*. 2002;120:797-803.
- Ahmed FA, Hegazy K, Chaudhary P, Sharma SC. Neuroprotective effect of alpha(2) agonist (brimonidine) on adult rat retinal ganglion cells after increased intraocular pressure. *Brain Res*. 2001;913:133-139.
- Yoles E, Schwartz M. Elevation of intraocular glutamate levels in rats with partial lesion of the optic nerve. *Arch Ophthalmol*. 1998;116:906-910.
- Lai RK, Chun T, Hasson D, Lee S, Mehrbod F, Wheeler L. Alpha-2 adrenoceptor agonist protects retinal function after acute retinal ischemic injury in the rat. *Vis Neurosci*. 2002;19:175-185.
- Lonngren U, Napankangas U, Lafuente M, et al. The growth factor response in ischemic rat retina and superior colliculus after brimonidine pre-treatment. *Brain Res Bull*. 2006;71:208-218.
- Saylor M, McLoon LK, Harrison AR, Lee MS. Experimental and clinical evidence for brimonidine as an optic nerve and retinal neuroprotective agent: an evidence-based review. *Arch Ophthalmol*. 2009;127:402-406.
- Wheeler L, WoldeMussie E, Lai R. Role of alpha-2 agonists in neuroprotection. *Surv Ophthalmol*. 2003;48(suppl 1):S47-S51.
- Koo H, Moon H, Han H, et al. The movement of self-assembled amphiphilic polymeric nanoparticles in the vitreous and retina after intravitreal injection. *Biomaterials*. 2012;33:3485-3493.
- Farjo KM, Ma JX. The potential of nanomedicine therapies to treat neovascular disease in the retina. *J Angiogenes Res*. 2010;2:21.
- Kim H, Robinson SB, Csaky KG. Investigating the movement of intravitreal human serum albumin nanoparticles in the vitreous and retina. *Pharm Res*. 2009;26:329-337.
- Kratz F. Albumin as a drug carrier: design of prodrugs, drug conjugates and nanoparticles. *J Control Release*. 2008;132:171-183.
- Prajapati KD, Sharma SS, Roy N. Current perspectives on potential role of albumin in neuroprotection. *Rev Neurosci*. 2011;22:355-363.
- Stanyon HF, Viles JH. Human serum albumin can regulate amyloid-beta peptide fiber growth in the brain interstitium: implications for Alzheimer disease. *J Biol Chem*. 2012;287:28163-28168.
- Langer K, Balthasar S, Vogel V, Dinauer N, von Briesen H, Schubert D. Optimization of the preparation process for human serum albumin (HSA) nanoparticles. *Int J Pharm*. 2003;257:169-180.
- Sarikcioglu L, Demir N, Demirtop A. A standardized method to create optic nerve crush: Yasargil aneurysm clip. *Exp Eye Res*. 2007;84:373-377.
- Wadhwa S, Paliwal R, Paliwal SR, Vyas SP. Hyaluronic acid modified chitosan nanoparticles for effective management of glaucoma: development, characterization, and evaluation. *J Drug Target*. 2010;18:292-302.
- Grove K, Dobish J, Harth E, Ingram MC, Galloway RL, Mawn LA. Trans-meningeal drug delivery to optic nerve ganglion cell axons using a nanoparticle drug delivery system. *Exp Eye Res*. 2014;118:42-45.
- Edelhauser HF, Rowe-Rendleman CL, Robinson MR, et al. Ophthalmic drug delivery systems for the treatment of retinal diseases: basic research to clinical applications. *Invest Ophthalmol Vis Sci*. 2010;51:5403-5420.
- Le Goff MM, Bishop PN. Adult vitreous structure and postnatal changes. *Eye (Lond)*. 2008;22:1214-1222.
- Nishihara H. [Studies on the ultrastructure of the inner limiting membrane of the retina-distribution of anionic sites in the inner limiting membrane of the retina]. *Nippon Ganka Gakkai Zasshi*. 1991;95:951-958.
- Bunt-Milam AH, Saari JC, Klock IB, Garwin GG. Zonulae adherentes pore size in the external limiting membrane of the rabbit retina. *Invest Ophthalmol Vis Sci*. 1985;26:1377-1380.
- Desai N, Trieu V, Yao Z, et al. Increased antitumor activity, intratumor paclitaxel concentrations, and endothelial cell transport of cremophor-free, albumin-bound paclitaxel, ABI-007, compared with cremophor-based paclitaxel. *Clin Cancer Res*. 2006;12:1317-1324.
- Siddiqui SS, Siddiqui ZK, Malik AB. Albumin endocytosis in endothelial cells induces TGF-beta receptor II signaling. *Am J Physiol Lung Cell Mol Physiol*. 2004;286:L1016-L1026.
- Ivens S, Kaufer D, Flores LP, et al. TGF-beta receptor-mediated albumin uptake into astrocytes is involved in neocortical epileptogenesis. *Brain*. 2007;130:535-547.
- Diebold Y, Calonge M. Applications of nanoparticles in ophthalmology. *Prog Retin Eye Res*. 2010;29:596-609.

33. Elzoghby AO, Samy WM, Elgindy NA. Albumin-based nanoparticles as potential controlled release drug delivery systems. *J Control Release*. 2012;157:168-182.
34. Bohrmann B, Tjernberg L, Kuner P, et al. Endogenous proteins controlling amyloid beta-peptide polymerization. Possible implications for beta-amyloid formation in the central nervous system and in peripheral tissues. *J Biol Chem*. 1999;274:15990-15995.
35. Milojevic J, Melacini G. Stoichiometry and affinity of the human serum albumin-Alzheimer's A $\beta$  peptide interactions. *Biophys J*. 2011;100:183-192.
36. Guo L, Salt TE, Luong V, et al. Targeting amyloid-beta in glaucoma treatment. *Proc Natl Acad Sci U S A*. 2007;104:13444-13449.
37. Krishnamoorthy RR, Clark AF, Daudt D, Vishwanatha JK, Yorio T. A forensic path to RGC-5 cell line identification: lessons learned. *Invest Ophthalmol Vis Sci*. 2013;54:5712-5719.
38. Van Bergen NJ, Wood JP, Chidlow G, et al. Recharacterization of the RGC-5 retinal ganglion cell line. *Invest Ophthalmol Vis Sci*. 2009;50:4267-4272.
39. Ahmed Z, Kalinski H, Berry M, et al. Ocular neuroprotection by siRNA targeting caspase-2. *Cell Death Dis*. 2011;2:e173.
40. Magharious M, D'Onofrio PM, Hollander A, Zhu P, Chen J, Koeberle PD. Quantitative iTRAQ analysis of retinal ganglion cell degeneration after optic nerve crush. *J Proteome Res*. 2011;10:3344-3362.